#### **CONFERENCE PRE-PRINT**

# FIRST FAST ION MEASUREMENTS BY THE COLLECTIVE THOMSON SCATTERING AND ION CYCLOTRON EMISSION DIAGNOSTICS AT WENDELSTEIN 7-X.

# Results from the OP 2.3 experimental campaign

D. Moseev, S. Ponomarenko, R. Ochoukov, P. Aleynekov, D. Hartmann, J.-P. Kallmeyer, L. Krier, I. Kuzmych, H.P. Laqua, S. Marsen, T. Schröder, T. Stange, R.C. Wolf Max-Planck Institute for Plasma Physics Greifswald and Garching, Germany Email: dmitry.moseev@ipp.mpg.de

#### M. Dreval

Institute of Plasma Physics, National Science Center, Kharkov Institute of Physics and Technology 61108 Kharkov, Ukraine

K. Crombé, Ye.O. Kazakov, J. Ongena, B.C.G. Reman, B. Schweer, I. Stepanov Laboratory for Plasma Physics, LPP-ERM/KMS, TEC Partner 1000 Brussels, Belgium

#### R.O. Dendy

Centre for Fusion, Space and Astrophysics, University of Warwick Coventry CV47AL, UK

K.G. McClements, O. Samant United Kingdom Atomic Energy Authority, Culham Campus Abingdon, Oxfordshire, UK

S.K. Nielsen, R. Ragona, J. Rasmussen, M. Salewski Department of Physics, Technical University of Denmark Kgs. Lyngby 2800, Denmark

#### B.S. Schmidt

University of California Irvine, Department of Physics and Astronomy Irvine, CA, US 92697

#### Abstract

In this paper we present the first measurements of the fast-ion-driven ion cyclotron emission (ICE) measured by the B-dot probes installed in the min-B cross-section of the stellarator and by a strap of the ICRF antenna, installed in the max-B cross-section of the stellarator. We report here on the dependence of ICE intensity on the magnetic configurations, the first measurements of the global Alfvén eigenmode (GAE) and a core-localized ICE. The first measurements of 174 GHz collective Thomson scattering measurements are also presented, including the spectra during the short pulses of NBI.

#### IAEA-CN-392/INDICO ID

#### 1. INTRODUCTION

Wendelstein 7-X (W7-X) is an optimized stellarator with five-fold toroidal symmetry. A key design criterion of this quasi-isodynamic reactor was improved fast-ion confinement in high-beta regimes. To verify this optimization, a broad set of fast-ion diagnostics is required. Here we present results from two diagnostics at W7-X: collective Thomson scattering (CTS), which measures confined fast ions, and ion cyclotron emission (ICE), which probes mainly lost ions.

ICE denotes electromagnetic or electrostatic fluctuations at frequencies of about  $10^{-1}$ – $10^{1}$  times the ion cyclotron frequency. It is usually driven by fast ions through the magnetoacoustic cyclotron instability (MCI) or by high-frequency Alfvén eigenmodes (AE). ICE can also appear in plasmas without energetic ions, termed thermal population ICE (TPICE). MCI is often linked to fast-ion losses. Because ICE is sensitive to distribution functions with sharp positive gradients in phase space, it can be used to detect fusion products, as found recently in ASDEX Upgrade, KSTAR, and LHD. We report the first observation of fast-ion-driven ICE in W7-X.

CTS measures microwave radiation scattered from plasma fluctuations. For a Salpeter parameter  $\alpha > 1$  [1], the diagnostic is sensitive to collective fluctuations, in particular perturbations of electron density and magnetic fields induced by ion motion. A detailed description of the method is given in the review [2]. The diagnostic is currently also being used on ASDEX Upgrade [3, 4], LHD [5, 6], GDT trap [7, 8], is proposed for ITER and SPARC [9, 10], and is used for diagnosing local plasma parameters in laser-produced high energy density plasmas [11, 12].

The paper is structured as follows. Section 2 shows CTS findings. Section 3 presents ICE results. Section 4 gives the conclusions.

## 2. COLLECTIVE THOMSON SCATTERING MEASUREMENTS

The CTS diagnostic at W7-X originally operated using 140 GHz gyrotron as a source of probing radiation. It was one of the gyrotrons that are used for the second harmonic electron cyclotron resonance heating (ECRH). Although this choice allowed to demonstrate technical capabilities of the system [13], due to strong noise from the electron cyclotron emission at around 140 GHz, the diagnostic was moved to a new frequency, 174 GHz [14, 15]. The measurements can be done both at the min-B (triangular) and max-B (bean-shaped) cross-sections of the machine. In this preprint, we report the results obtained in the bean-shaped cross-section of W7-X.

The CTS receiver is a single heterodyne radiometer, where the RF scattering signal coming from the quasi-optical transmission line is collected through a broadband horn. The RF signal, being filtered by the band-pass filters to avoid aliasing and by the notch filtered to block stray radiation from the gyrotron, is amplified by a 25 dB low-noise amplifier (LNA). The filters are followed by the actively controlled voltage-controlled attenuator and an isolator before the 176 GHz RF mixer. The mixed-down signal in the frequency range 0 - 6 GHz is further filtered through low-pass filter and amplified, before being sampled with a 12.5 GS/s 8 analog-to-digital converter with 5 GHz analog bandwidth. More detailed description of the receiver can be found in the literature [16].

The front-end steering antennas from the gyrotron launcher were used to both launch the 174 GHz probing beam at the power of about 200 kW, and to receive the scattering radiation into the radiometer. In order to avoid multiple overlaps of the receiver beam with the reflections of the probing gyrotron beam, the gyrotron fired into a specially designed tile on the opposite side of the vacuum vessel. The tile has pyramidal structures on its surface, that scatter the oncoming directed beam into a large solid angle, basically converting it into stray radiation radiation.

The scattering geometry is chosen such that the wave vector of the resolved fluctuations,  $\mathbf{k}^{\delta} = \mathbf{k}^{s} - \mathbf{k}^{i}$ , where  $\mathbf{k}^{s}$  and  $\mathbf{k}^{i}$  denote the wave vectors of the scattered and incident radiation, respectively, is nearly perpendicular to the magnetic field in the plasma. In such a geometry, the scattering spectrum also contains information on the ion cyclotron motion, which allows studying plasma composition [17].

Figure 1 shows two scattering spectra from the W7-X experiment 20250514.52. Those spectra are taken slightly off-axis, at the normalized radius of 0.3 in the nearly perpendicular geometry with the angle  $\phi = \angle(\mathbf{k}^{\delta}, \mathbf{B}) = 92^{\circ}$ . This gives rise to the ion cyclotron feature in the spectrum with the spacing of  $\approx 35$  MHz, which corresponds to the ion cyclotron frequency of hydrogen in the location of the measurements. Spectroscopy measurements at the plasma edge also confirm almost pure hydrogen plasma.

A peak at 173.4 GHz is a spurious mode of the gyrotron.

The short pulses of NBI with the NBI source S8 probably triggers a lower hybrid instability, which was previously observed in CTS spectra on Wendelstein 7-AS [18], TEXTOR, and ASDEX Upgrade [19]. We consider it unlikely that the observed feature is a direct signature of the NBI fast-ion population, i.e. a feature that originates from the projected fast-ion velocity distribution itself. Instead, we argue that it is a secondary effect, caused by the instability excited by the fast ions:

• Only a single peak is detected on the CTS spectra. NBI at W7-X has three energy components: 55 keV, 27.5 keV and

18 keV. EAch of the energy components is significant and all of the peaks should be pronounced.

- Should the fast ion population have a direct detectable influence on the scattering spectrum, their contribution must be nearly symmetrical with respect to the gyrotron frequency due to the chosen scattering geometry.
- The density of fast ions is too small from a single short pulse from one NBI source.

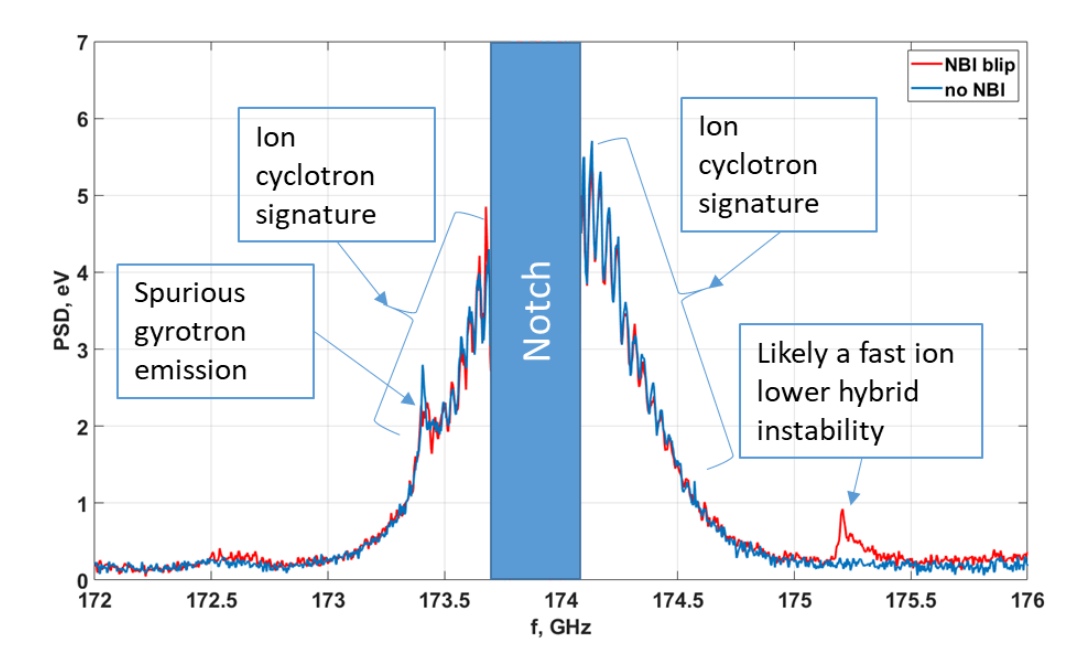


FIG. 1. CTS spectra from W7-X experiment 20250514.52. Red curve shows the measurements during the short pulse of NBI from the source S8, blue curve is a spectrum taken during the NBI off phase.

## 3. ION CYCLOTRON EMISSION MEASUREMENTS

ICE measurements are conducted at two spatially different locations. The first one is in the max-B cross-section in module 3 (out of 5), it is an unshielded strap of the ICRF antenna [20]. The ICRF strap is sensitive both to the electrostatic and electromagnetic fluctuations since it does not have a Faraday shield in front of it.

There are additionally four B-dot probes installed at the min-B cross-section of W7-X in module 1 at the CTS heatshield [21]. A sketch with the relative locations of the diagnostic is shown in figure 2.

The ICRF strap is connected to the 1 GS/s 14 bit ADC using 75 m Ultraflex-10 triaxial cable and a 10 dB attenuator via a measurement insert terminal.

Fast-ion-driven ICE is not observed in every magnetic configuration of Wendelstein 7-X. Typically, ICE is detected in all discharges in the standard configuration and in the low-mirror configuration. However, in the high-mirror and low-shear configurations, practically no ICE signatures were observed, or it is orders of magnitude weaker than in the experiments in standard or low-mirror configuration.

Typically, edge ICE is caused by fast ions which create a ring distribution in the velocity space and drive MCI unstable, and that was predicted for W7-X [22]. This mechanism implies that the strength of the instability driving the ICE depends on the energy of the NBI ions in combination with the orientation of the NBI beam with respect to the local magnetic field direction. We choose two W7-X experiments with similar plasma parameters and the same NBI source used for the charge-exchange diagnostic. Figure 3 shows two discharges, one is 20250403.79 in the standard magnetic field configuration and the magnetic field of 2.52 T on two left panels, and another one is 20250306.65 also in the same standard configuration and the inverted magnetic field of -2.52 T. The power of ICE in the reversed field configuration is several times higher, which could be explained by higher fast ion losses due to initially unfavorable grad-B drift direction of freshly ionized ions. The spectrogram reveals, that the experiment 20250306.65, conducted in the reversed field configuration, completely lacks a peak at the second harmonic of ICE. In order to have a closer look at the harmonics, we show time-averaged spectra of the first nine ion cyclotron harmonics in figure 4. The averaging is done over one short pulse of NBI. For the direct field case (20250403.79) the averaging is done in the period t = [5.5, 5.55] s. For the reversed field measurements (20250306.65) the averaging window was t = [2.1, 2.15] s. In both cases, fundamental harmonics is the strongest. The lower harmonics, the first, third and fourth, cover roughly the

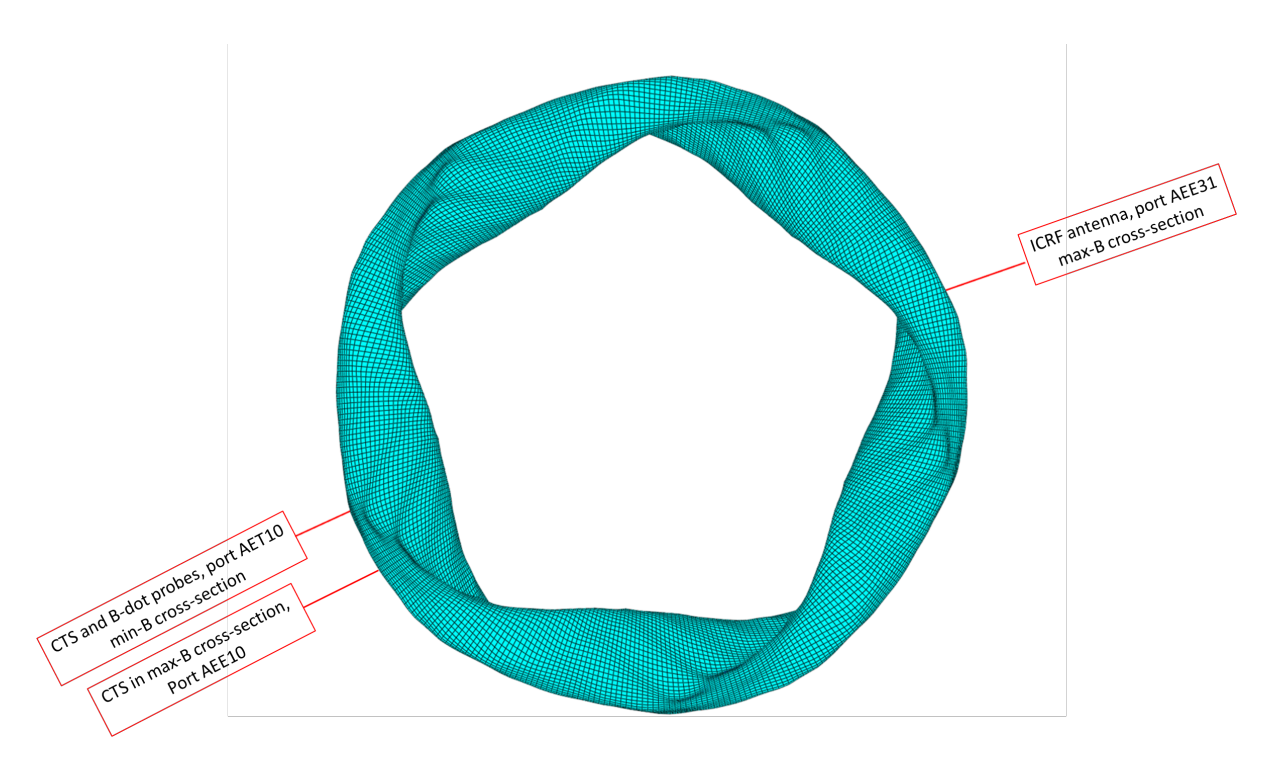


FIG. 2. Top view of Wendelstein 7-X with indicated locations of the diagnostic.

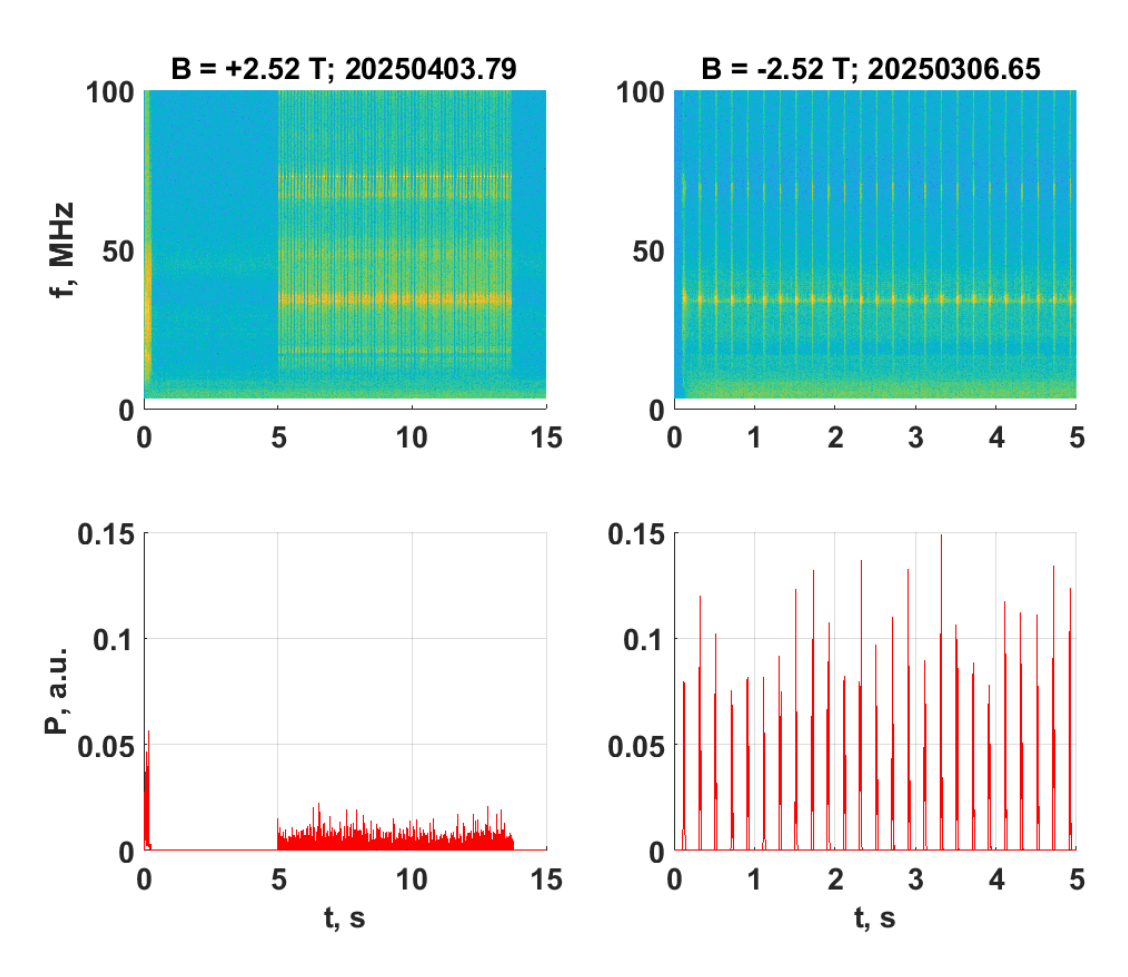


FIG. 3. Upper panels: spectrograms of ICE in the W7-X experiments 20250403.79 and 20250306.65 from left to right, respectively. Bottom panels show the corresponding power of the ICE signals, picked up by the ICRF strap.

same bandwidth. From the sixth harmonic, the direct field experiment has frequencies that are consistently shifted to the lower frequencies.

It is interesting to compare signals from the ICRF strap with the data obtained by the B-dot probe. According to the theoret-

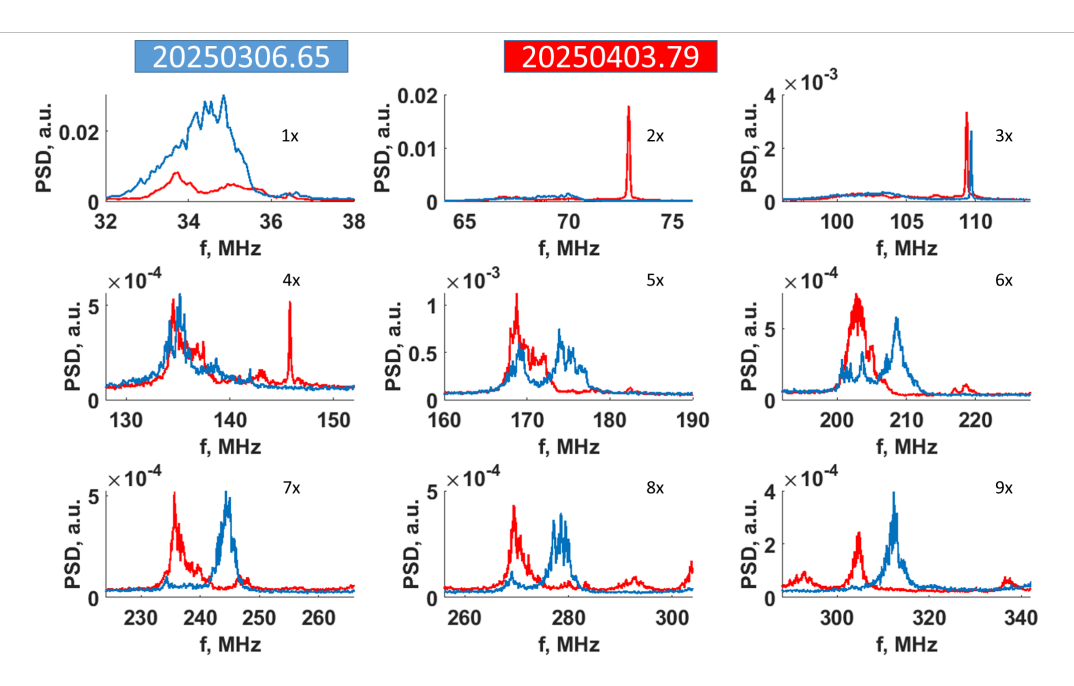


FIG. 4. First nine harmonics of the ion cyclotron emission in the W7-X experiments 20250403.79 (red curve) and 20250306.65 (blue curve).

ical investigation [22], the first harmonics of ICE should be predominantly of electromagnetic nature, while the electrostatic fluctuations dominate in the higher harmonics. We investigate the same discharge 20250403.79, which was conducted in the standard configuration with the magnetic field on axis at the max-B cross-section of 2.52 T. Figure 5 shows first nine harmonics of ICE measured by the ICRF strap (blue), toroidal B-dot probe (red), and poloidal B-dot probe (black). The spectra are on a linear scale and are time-averaged over 50 ms ( $t = [5.5 \ 5.55]$  s). The B-dot spectra are scaled by factor 50. Firstly, in contrast to the thermal population ICE in W7-X [23], where the signal was detected solely on the ICRF strap, the fast-ion-driven ICE is visible on all the detectors, although its signatures are different depending on the type of the detector.

Firstly, when watching at the first harmonic, we should note that all three spectra cover the same frequency range, although the ICRF strap and the B-dot probes are separated toroidally by approximately  $150^{\circ}$  and are located at the regions with different magnetic strength and topology. This indicates that the signal has a common origin, which is likely located along the neutral beam path.

Both first and second harmonic signatures look very similar, which indicates that they have an electromagnetic nature and a small (if any) electrostatic component. The third harmonic is strongly pronounced on the strap but is weakly visible on the B-dot probes. On the B-dot probes it is several times stronger on the poloidally oriented probe. Strong spectral lines at 220 MHz and 320 MHz on the poloidal B-dot probe are due to the electronic issues and not related to the NBI. The fact that the signal from the ICRF strap persists to exist at higher harmonic numbers and vanishes on the B-dot probe is in agreement with the numerical investigation of ICE in W7-X [22], where it was found that the higher harmonics of ICE should be of electrostatic nature, to which B-dot probes are not sensitive.

## 4. CONCLUSIONS

The CTS diagnostic at 174 GHz is fully commissioned in the bean-shaped cross-section of W7-X. The diagnostic can be used for inferring the bulk ion parameters, such as ion temperature and plasma composition. It is also sensitive to the fast-ion-driven instabilities. So far the fast ion density was too small to measure the contribution of the projection of the velocity distribution function directly in the fast ion experiments with CTS, but given a very high signal-to-noise ratio it should be possible. It should be noted that the good signal-to-noise ratio is achievable at electron temperatures below 5 keV, otherwise the level of electron cyclotron emission from relativistically downshifted electrons gets too high.

Fast-ion-driven ICE is regularly observed at W7-X on both the ICRF strap and on the B-dot probes, in contrast to the thermal population ICE, which is detectable exclusively on the ICRF strap. Spectra, obtained from different toroidal locations with

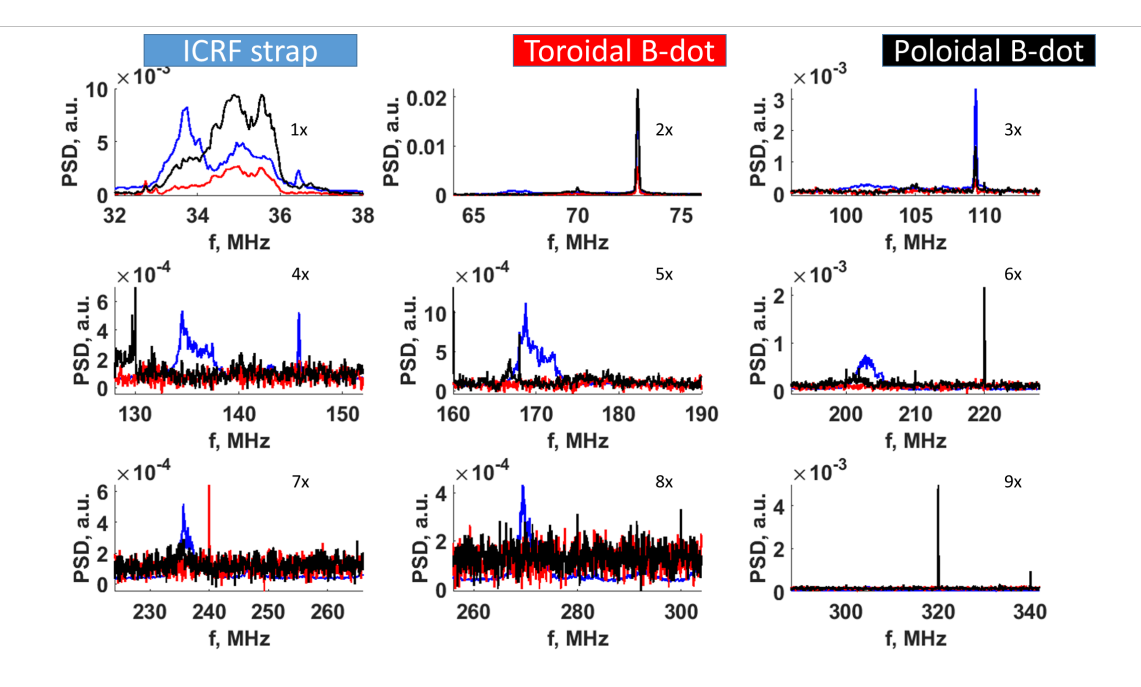


FIG. 5. Comparison of the ICRF strap and the B-dot probe measurements in the W7-X discharge 20250403.79. Blue curves show the ICRF strap measurements; red and black curves show the measurements from the B-dot probes with toroidal and poloidal polarization, respectively. The B-dot PSD is scaled by a factor of 50 in order to be compared with the ICRF strap measurements.

different magnetic field topology, cover the same frequency range, which indicates a common origin of the detected signal. This location is likely to be along the neutral beam path.

The signal from the B-dot probes is very similar to the signal on the ICRF strap on the first three harmonics, however for the higher harmonic numbers it only exists on the ICRF strap. This agrees well with the previous numerical study of ICE at W7-X, where it was predicted that low harmonic numbers are of electromagnetic nature and have to be observed by both types of detectors, while high harmonics are of electrostatic nature and could only be seen by the unscreened ICRF strap.

We notice, that fast-ion-driven ICE is strongly dependent on the magnetic field configuration. The exact reason for it is yet unknown.

### ACKNOWLEDGEMENTS

This work has been carried out within the framework of the EUROfusion Consortium, funded by the European Union via the Euratom Research and Training Programme (Grant Agreement No 101052200 — EUROfusion). Views and opinions expressed are however those of the author(s) only and do not necessarily reflect those of the European Union or the European Commission. Neither the European Union nor the European Commission can be held responsible for them.

## REFERENCES

- [1] E E Salpeter. Electron density fluctuations in a plasma. *Physical Review*, 120:1528, 1960.
- [2] D Moseev, M Salewski, M Garcia-Muñoz, B Geiger, and M Nocente. Recent progress in fast-ion diagnostics for magnetically confined plasmas. Reviews of Modern Plasma Physics, 2:7, 12 2018.
- [3] J Rasmussen, S K Nielsen, M Stejner, B Geiger, M Salewski, A S Jacobsen, S B Korsholm, F Leipold, P K Michelsen, D Moseev, M Schubert, J Stober, G Tardini, and D Wagner. Consistency between real and synthetic fast-ion measurements at asdex upgrade. *Plasma Physics and Controlled Fusion*, 57:75014, 7 2015.
- [4] S K Nielsen, M Stejner, J Rasmussen, A S Jacobsen, S B Korsholm, F Leipold, M Maraschek, F Meo, P K Michelsen, D Moseev, M Salewski, M Schubert, J Stober, W Suttrop, G Tardini, and D Wagner. Measurements of the fast-ion distribution function at asdex upgrade by collective thomson scattering (cts) using active and passive views. *Plasma Physics and Controlled Fusion*, 57:35009, 3 2015.

- [5] M Nishiura, S Kubo, K Tanaka, R Seki, S Ogasawara, T Shimozuma, K Okada, S Kobayashi, T Mutoh, K Kawahata, T Watari, L H D Experiment Group, T Saito, Y Tatematsu, S B Korsholm, and M Salewski. Spectrum response and analysis of 77 ghz band collective thomson scattering diagnostic for bulk and fast ions in lhd plasmas. *Nuclear Fusion*, 54:023006, 2014.
- [6] Masaki Nishiura, Shun Adachi, Kenji Tanaka, Shin Kubo, Naoki Kenmochi, Takashi Shimozuma, Ryoma Yanai, Teruo Saito, Hideo Nuga, and Ryosuke Seki. Collective thomson scattering diagnostic with in situ calibration system for velocity space analysis in large helical device. Review of Scientific Instruments, 93:053501, 5 2022.
- [7] A G Shalashov, E D Gospodchikov, T A Khusainov, L V Lubyako, A L Solomakhin, and D V Yakovlev. First results of collective thomson scattering diagnostic of fast ions at the gdt open magnetic trap. *Physics of Plasmas*, 29:80702, 2022.
- [8] A G Shalashov, E D Gospodchikov, L V Lubyako, T A Khusainov, E A Shmigelsky, E I Soldatkina, and A L Solomakhin. Progress using collective thomson scattering of microwave radiation to detect fast ions and plasma instabilities at the gdt open magnetic trap. *Physics of Plasmas*, 31:122506, 12 2024.
- [9] S B Korsholm, A Chambon, B Gonçalves, V Infante, T Jensen, M Jessen, E B Klinkby, A W Larsen, R Luis, Y Nietiadi, E Nonbøl, J Rasmussen, D Rechena, M Salewski, A Taormina, A Vale, P Varela, L Sanchez, R M Ballester, V Udintsev, and Y Liu. Iter collective thomson scattering—preparing to diagnose fusion-born alpha particles (invited). Review of Scientific Instruments, 93:103539, 2022.
- [10] Mads Mentz-Jørgensen, Riccardo Ragona, Søren B Korsholm, and Jesper Rasmussen. Physics feasibility study of a collective thomson scattering diagnostic for sparc. *Nuclear Fusion*, 65:046028, 2025.
- [11] T Morita, Y Sakawa, K Tomita, T Ide, Y Kuramitsu, K Nishio, K Nakayama, K Inoue, T Moritaka, H Ide, M Kuwada, K Tsubouchi, K Uchino, and H Takabe. Thomson scattering measurement of a shock in laser-produced counter-streaming plasmas. *Physics of Plasmas*, 20:092115, 9 2013.
- [12] K Sakai, S Isayama, N Bolouki, M S Habibi, Y L Liu, Y H Hsieh, H H Chu, J Wang, S H Chen, T Morita, K Tomita, R Yamazaki, Y Sakawa, S Matsukiyo, and Y Kuramitsu. Collective thomson scattering in non-equilibrium laser produced two-stream plasmas. *Physics of Plasmas*, 27:103104, 10 2020.
- [13] D Moseev, M Stejner, T Stange, I Abramovic, H P Laqua, S Marsen, N Schneider, H Braune, U Hoefel, W Kasparek, S B Korsholm, C Lechte, F Leipold, S K Nielsen, M Salewski, J Rasmussen, M Weißgerber, and R C Wolf. Collective thomson scattering diagnostic at wendelstein 7-x. *Review of Scientific Instruments*, 90:13503, 1 2019.
- [14] L Krier, I Gr. Pagonakis, K A Avramidis, G Gantenbein, S Illy, J Jelonnek, J Jin, H P Laqua, A Marek, D Moseev, M Thumm, and W7-X Team. Theoretical investigation on possible operation of a 140 ghz 1 mw gyrotron at 175 ghz for cts plasma diagnostics at w7-x. *Physics of Plasmas*, 27:113107, 2020.
- [15] D Moseev, H P Laqua, T Stange, I Abramovic, S K Nielsen, S Äkäslompolo, K Avramidis, H Braune, G Gantenbein, S Illy, J Jelonnek, J Jin, W Kasparek, L Krier, S B Korsholm, C Lechte, A Marek, S Marsen, M Nishiura, I Pagonakis, M Salewski, J Rasmussen, A Tancetti, M Thumm, and R C Wolf. Collective thomson scattering diagnostic for wendelstein 7-x at 175 ghz. *Journal of Instrumentation*, 15:C05035–C05035, 2020.
- [16] S. Ponomarenko, D. Moseev, T. Stange, L. Krier, P. Stordiau, H. Braune, G. Gantenbein, J. Jelonnek, A. Kuleshov, H. P. Laqua, C. Lechte, S. Marsen, S. K. Nielsen, J. W. Oosterbeek, B. Plaum, R. Ragona, J. Rasmussen, T. Ruess, M. Salewski, M. Thumm, and J. Zimmermann. Development of the 174 ghz collective thomson scattering diagnostics at wendelstein 7-x. Review of Scientific Instruments, 95, 1 2024.
- [17] S B Korsholm, M Stejner, H Bindslev, V Furtula, F Leipold, F Meo, P K Michelsen, D Moseev, S K Nielsen, M Salewski, M de Baar, E Delabie, M Kantor, and A Bürger. Measurements of intrinsic ion bernstein waves in a tokamak by collective thomson scattering. *Phys. Rev. Lett.*, 106:165004, 4 2011.
- [18] A G Shalashov, E V Suvorov, L V Lubyako, and H Maassberg. Nbi-driven ion cyclotron instabilities at the w7-as stellarator. *Plasma Physics and Controlled Fusion*, 45:395–412, 4 2003.
- [19] D Moseev. Fast Ion Dynamics in ASDEX Upgrade and TEXTOR Measured by Collective Thomson Scattering. PhD thesis, November 2011.
- [20] J Ongena, D Castano-Bardawil, K Crombé, Y O Kazakov, B Schweer, I Stepanov, M Van Schoor, M Vervier, A Krämer-Flecken, O Neubauer, D Nicolai, G Satheeswaran, G Offermanns, K P Hollfeld, A Benndorf, A Dinklage, D Hartmann, J P Kallmeyer, R C Wolf, and TEC. Physics design, construction and commissioning of the icrh system for the stellarator wendelstein 7-x. Fusion Engineering and Design, 192:113627, 2023.

## IAEA-CN-392/INDICO ID

- [21] D Moseev, R Ochoukov, V Bobkov, R O Dendy, H Faugel, D Hartmann, J.-P. Kallmeyer, J Lansky, H P Laqua, S Marsen, K G McClements, S K Nielsen, A Reintrog, M Salewski, B S Schmidt, T Schulz, and T Stange. Development of the ion cyclotron emission diagnostic for the w7-x stellarator. *Review of Scientific Instruments*, 92:33546, 2021.
- [22] O Samant, R O Dendy, S C Chapman, D Moseev, and R Ochoukov. Predicting ion cyclotron emission from neutral beam heated plasmas in wendelstein7-x stellarator. *Nuclear Fusion*, 64:056022, 2024.
- [23] D Moseev, R Ochoukov, M Dreval, I Kuzmych, P Aleynikov, K Aleynikova, S Bozhenkov, R O Dendy, D Hartmann, J.-P Kallmeyer, Ye O Kazakov, L Krier, H P Laqua, S Marsen, K G Mcclements, J Ongena, J W Oosterbeek, S Ponomarenko, B Reman, J Riemann, M Salewski, O Samant, D Straus, B S Schmidt, T Schröder, B Schweer, T Stange, R C Wolf, J Zimmermann, and W7-X Team. Ion cyclotron emission from ecrh-heated plasmas in wendelstein 7-x. submitted to Physics of Plasmas, 2025.